Thermochimica Acta, 20 (1977) 141–175
© Elsevier Scientific Publishing Company, Amsterdam – Printed in The Netherlands

A COMPACT DIFFERENTIAL ISOPERIBOL CALORIMETER WITH VARIABLE HEAT SHIELDS

ALAN E. VAN TIL* AND DENNIS C. JOHNSON
Department of Chemistry, Iowa State University, Ames, Iowa 50011 (U.S.A.)
(Received 23 September 1976)

ABSTRACT

The dynamic characteristics of an isoperibol solution calorimeter with electrical heating are discussed on a theoretical basis.

The design requirements of a solution calorimeter are briefly reviewed. A calorimeter which satisfies these requirements was constructed and is described here. The dynamics of solution heating by an electrical heater are mathematically developed and computer generated heating curves are compared to experimental curves.

INTRODUCTION

Traditionally, calorimeters have been divided into adiabatic and isothermal (isoperibol) types with the distinction being related to the manner of temperature control of the environment of the calorimeter. The preferred method for maintaining a uniform temperature environment around the calorimeter involves the so-called "submarine" technique in which the calorimeter cell is submerged in a tank containing a thermostated liquid with mechanical stirring. A second method used only for isothermal calorimetry employs a thick insulating jacket, usually of a plastic foam, around the cell. White[1], in his classic text on calorimetry, treated in detail many other aspects of solution calorimetry. A recent review by Churney et al.[2] further defined the requirements of solution calorimetry. In these references, transient behavior and the dynamics of the change in bulk solution temperature during and immediately after the main period of heating are ignored. Ignorance of the response dynamics can lead to erroneous application of solution calorimetry especially in the study of reaction kinetics. Here, we describe a calorimeter which is sufficiently compact for use in a fume hood, is operable with readily available temperature controllers, and is sufficiently stable to permit 2–6 parts-per-thousand precision for measurement of total energy change in the range of 5–15 cal. A theoretical examina-

---

* Present address: Corporate Research, UOP Inc., Des Plaines, Ill. 60016, (U.S.A.). Author to whom correspondence should be sent.

tion of the dynamic response of the solution bulk temperature to electrical heating is given using linear methods to obtain a useful mathematical solution.

Solution calorimetry is a diversified area of research and standardization of equipment design has not yet been attained[3]. This results, no doubt, from differing requirements and opinions of the workers involved. Sunner and Wadsö[4] discussed the general requirements of isoperibol calorimeters. Christensen et al.[5] elaborated on these requirements and a commercial unit was constructed according to their design[6]. Both groups of workers decided early that a submarine isoperibol calorimeter is best suited for solution calorimetry of short duration (< 1 h). Sunner and Wadsö came to the correct conclusion that the design of the calorimeter lid has a great affect on the dynamic calorimetric behavior. Christensen et al.[7] apparently also experienced difficulty in obtaining a uniform temperature field above the solution as witnessed by the lid modification proposed. Two factors are of special importance in lid design: the means for attaining a uniform temperature field across the lid and the method by which mounting probes can be suspended into the calorimeter vessel so that heat conduction along the probes is minimized. If materials with low thermal conductivity are used for the entire calorimeter lid, large radial temperature gradients can develop even when the lid is submerged with the cell in a constant temperature bath. The quantity of heat flowing into or out of the solution in the cell via the probes depends on the type of material in contact with the solution and the total submerged area. The volume of the submerged portions of the probes will also affect the dynamic response of the solution temperature because of interference with convective heat transport in the solution. A very low heat-loss modulus was reported by Christensen et al.[5] which undoubtedly resulted from their use of Teflon tubing around probes into the solution and their efforts to miniaturize the probes.

We suggest two requirements for the design of solution calorimeters in addition to the five given by Sunner and Wadsö[4]: (1) Mixing of the solution in the calorimeter should be uniformly turbulent throughout the bulk; (2) bulk solution evaporation and uptake of gases from the vapor space above the solution should be minimized.

Popular stirring devices are propellers, magnetic stirring bars, and vibrating rods. Problems common to the first two types are vortex formation and spraying of the solution onto the calorimeter walls and lid at high stirring speeds. Highly volatile or toxic materials must be handled in a completely closed system for which magnetic stirring is the only option. Stirring by a smooth rotating disk has not been discussed although it was apparently used by Johansson[8]. It is our experience that a rotating disk provides rapid solution stirring, and a uniform flow pattern around a thermistor placed just below the plane of the disk. We have found that positioning the disk at a depth of $\frac{3}{4}\, l_b$ provides adequate stirring with no vortex formation, minimal gas uptake, and no spraying. It is a common misconception that a great amount of visible surface disruption is indicative of rapid solution mixing. The movement of a large volume of fluid is also not equivalent to efficient mixing. Needed is uniform turbulent flow such that eddies are small and, hence, thermal and mass diffusion can be effective for eliminating spatial discontinuities in temperature and concentration. As expected, a compromise must be reached between efficient stirring and the maximum heat of stirring which can be tolerated.

Concurrent with mixing is the interaction of the bulk solution in the calorimeter cell with the vapor space above the solution. White[1] stressed that the calorimeter lid should be slightly warmer than the solution in the calorimeter cell to eliminate condensation of solvent vapors. Minimization of the volume of vapor space is also important especially for highly volatile solvents. The elimination of CO_2 adsorption by the solution has long been recognized as a difficult problem. Frequently, excess base is added to decrease the effect when pH change is not critical. It is our experience from electroanalytical studies with a rotating disc electrode that exclusion of O_2 is more difficult in cylindrical cells with flat bottoms rather than spherical cells. This can be understood from a study of the fluid-flow patterns in the two cell shapes and the consequential degree of disruption of the solution surface. Cells used in this work had round bottoms.

THEORETICAL

Our consideration proceeds from the work of Polaczek and Lisicki[9]. Their key simplifying assumption was the combining of heat capacity and heat transfer characteristics of the probes with those of the cell wall. In practice, the surface area of the probes in contact with the bulk solution may nearly equal the area of the cell wall but the heat capacity of the probes cannot be determined independent of the cell wall in the single apparatus. In this work, the separate heat transfer coefficients of the probes and wall are used with the combined heat capacity to calculate the time constant for the cell wall. A second new consideration here is that the time constant of mixing, τ_m, is the value determined according to Brodkey[10] at r, the distance from the cell's vertical axis to the electrical heater. The bulk solution temperature, T_b, is usually considered to be uniform throughout the solution except in the boundary layer of the electrical heater. The boundary layer temperature, T_{bl}, is equal to T_b before heating but is greater than T_b during heating. The third new consideration is a correction for spatial inhomogeneity of T_b within the calorimeter cell. This yields the "excess" temperature in the region of the temperature sensor.

General equation

The time response of the bulk solution temperature can be derived from the heat flux balance given by eqn (1)

$$h_h A_h(T_h - T_{bl}) = C_w \frac{dT_w}{dt} + C_b \frac{dT_b}{dt} + C_b \frac{d(T_{bl} - T_b)}{dt} \tag{1}$$

The combined heat capacity of the cell wall and stems is C_w and

$$C_w \frac{dT_w}{dt} = h_w A_w(T_b - T_w) \tag{2}$$

A time constant for the wall is defined as

$$\tau_w = \frac{C_w}{h_w A_w} \text{ with } Z_1 = \frac{1}{\tau_w} \tag{3}$$

Consideration of heat flux at the heater yields

$$\frac{dQ_h}{dt} = P_h = h_h A_h (T_h - T_{bl}) + C_h \frac{dT_h}{dt} \tag{4}$$

A time constant for the heater is defined as

$$\tau_h = \frac{C_h}{h_h A_h} \text{ with } Z_2 = \frac{1}{\tau_h} \tag{5}$$

The temperature difference $T_{bl} - T_b$ is expressed in terms of the time constant for mixing

$$T_{bl} - T_b = \tau_m \frac{dT_b}{dt} = \tau_m \gamma_b \tag{6}$$

with $Z_3 = \dfrac{1}{\tau_m}$

Combination of the Laplacian transforms of eqns (1), (2) and (4) yields eqn (7)

$$\left[\frac{h_h A_h}{C_h s + h_h A_h}\right] [sQ_h(s) - Q_h(0)] + \left[\frac{h_h A_h C_h}{C_h s + h_h A_h}\right] T_h(0)$$

$$+ h_h A_h \left[\frac{h_h A_h}{C_h s + h_w A_w} - 1\right] T_{bl}(s) = C_b[sT_b(s) - T_b(0)]$$

$$+ \left[\frac{C_w h_w A_w s}{C_w s + h_w A_w}\right] T_b(s) + C_w \left[\frac{C_w s}{C_w s + h_w A_w} - 1\right] T_w(0)$$

$$+ C_b \tau_m [s^2 T_b(s) - sT_b(0) - T_b'(0)] \tag{7}$$

An initial approximation is made that the $T_{bl}(s)$ term is negligible.

Solving eqn (7) for $T_b(s)$ yields eqn (8).

$$T_b(s) = \frac{Z_2 Z_3}{C_b} \left[\frac{(s + Z_1)}{s(s + Z_2)(s^2 + (Z_1 + Z_3)s + Z_1 Z_3(1 + C_w/C_b))}\right] \cdot$$

$$[sQ_h(s) - Q_h(0)] + \left[\frac{(s^2 + (Z_1 + Z_3)s + Z_1 Z_3)}{s(s^2 + (Z_1 + Z_3)s + Z_1 Z_3(1 + C_w/C_b))}\right] T_b(0)$$

$$+ \frac{C_w Z_1 Z_3}{C_b} \left[\frac{1}{s(s^2 + (Z_1 + Z_3)s + Z_1 Z_3(1 + C_w/C_b))}\right] T_w(0)$$

$$+ \left[\frac{(s + Z_1)}{s(s^2 + (Z_1 + Z_3)s + Z_1Z_3(1 + C_w/C_b))}\right] T_b'(0)$$

$$+ \frac{C_bZ_2Z_3}{C_b} \left[\frac{(Z_1 + s)}{s(Z_2 + s)(s^2 + (Z_1 + Z_3)s + Z_1Z_3(1 + C_w/C_b))}\right] T_h(0) \quad (8)$$

The total generated heat is

$$Q_h = P_h t \quad (9)$$

add the Laplacian transform of Q_h is

$$Q_h(s) = P_h/s^2 \quad (10)$$

Main period

The initial conditions for the main period of heating are

$t = 0$: $Q_h = 0$

$T_h = T_b = T_{bl} = 0$

$dT_b/dt = 0$

$T_w > T_b$

$0 < t \leq t_{cc}$: $Q_h = P_h t$

$T_h > T_{bl} > T_b$

$T_w \neq T_b$

At $t = 0$, the values of T_b for the two solutions in the differential calorimetric system are equal. For all values $t > 0$, the equality of T_b values no longer exists. The heat of stirring, γ_{stir}, and electrical heating of the solution by the thermistor, γ_{th}, are compensated for by use of a differential system. The remaining heat source is γ_{bkg} which results because $T_w > T_b$. Differences in heat exchange by the calorimeter's cells with the environment are compensated by use of trickle heaters initially adjusted when $t < 0$.

From the initial conditions, eqn (8) is written

$$T_b(s) = \frac{Z_2Z_3}{C_b} \left[\frac{(s + Z_1)}{s^2\{(s + Z_2)(s^2 + (Z_1 + Z_3)s + Z_1Z_3(1 + C_w/C_b))\}}\right] P_h$$

$$+ \frac{Z_1Z_3C_w}{C_b} \left[\frac{1}{s\{s^2 + (Z_1 + Z_3)s + Z_1Z_3(1 + C_w/C_b)\}}\right] T_w(0) \quad (11)$$

The denominators of the coefficients of P_h and $T_w(0)$ are characteristic of a second-order differential equation $\{s^2 + (Z_1 + Z_3)s + Z_1Z_3(1 + C_w/C_b)\}$ typically encountered for RLC circuits. The roots of the equation are

$$s = -\left(\frac{Z_1 + Z_3}{2}\right) \pm \left[\left(\frac{Z_1 + Z_3}{2}\right)^2 - Z_1Z_3(1 + C_w/C_b)\right]^{1/2} \quad (12)$$

Depending on the values of Z_1, Z_3 and C_w/C_b, the roots may be real or complex. Three cases result with three corresponding expressions for eqn (12).

Case I: The condition of underdamping exists when

$$\left(\frac{Z_1 + Z_3}{2}\right)^2 < Z_1 Z_3 (1 + C_w/C_b) \tag{13}$$

The coefficient of P_k can be factored as

$$\frac{K_1}{s} + \frac{K_2}{(s + Z_2)} + \frac{K_3}{(s + \alpha + \beta j)} + \frac{K_4}{(s + \alpha - \beta j)} \tag{14}$$

where

$$j = \sqrt{-1}$$

$$\alpha = \frac{Z_1 + Z_3}{2}$$

$$\beta = \left[Z_1 Z_3 (1 + C_w/C_b) - \left(\frac{Z_1 + Z_3}{2}\right)^2\right]^{1/2}$$

It is shown in ref. 11 that

$$K_1 = \frac{1}{C_b + C_w} \tag{15}$$

$$K_2 = \frac{Z_3(Z_1 - Z_2)}{Z_2[C_b(Z_2^2 - Z_2(Z_1 + Z_3)) + Z_1 Z_3 (C_b + C_w)]} \tag{16}$$

$$K_3 = r_1 \exp\{j\theta_1\} \tag{17}$$

$$K_4 = r_1 \exp\{-j\theta_1\} \tag{18}$$

where

$$r = [(a_1)^2 + (b_1)^2]^{1/2}$$

$$a = \frac{Z_2 C_b \beta [2\alpha\phi + (\beta^2 - \alpha^2)(Z_1 - Z_2)]}{Z_1 Z_3 \psi (C_b + C_w)^2}$$

$$b_1 = \frac{Z_2 C_b [\alpha^2 \phi + 2\alpha\beta^2 (Z_1 - Z_2) - \beta^2 \phi]}{Z_1 Z_3 \psi (C_b + C_w)^2}$$

$$\theta = \arcsin\{b_1/r_1\}$$

$$\phi = Z_1 Z_2 - (Z_1 + Z_2)\alpha + Z_1 Z_3 (1 + C_w/C_b)$$

$$\psi = 2Z_1[Z_2^2 - Z_2(Z_1 + Z_2) + Z_1 Z_3(1 + C_w/C_b)]\beta$$

The coefficient of the $T_w(0)$ term in eqn (11) is factored as

$$\frac{K_5}{s} + \frac{K_6}{s + \alpha + \beta j} + \frac{K_7}{s + \alpha - \beta j} \tag{19}$$

It is shown in ref. 11 that

$$K_5 = \frac{C_w}{C_b + C_w} \tag{20}$$

$$K_6 = r_2 \exp\{j\theta_2\} \tag{21}$$

$$K_7 = r_2 \exp\{-j\theta_2\} \tag{22}$$

where

$$r_2 = [(a_2)^2 + (b_2)^2]^{1/2}$$

$$a_2 = \frac{-C_w}{2(C_b + C_w)}$$

$$b_2 = \frac{-\alpha C_w}{2\beta(C_b + C_w)}$$

$$\theta_2 = \arcsin(b_2/r_2)$$

Finally, eqn (11) for $T_b(s)$ becomes

$$\begin{aligned} T_b(s) = {} & \left[\frac{1}{s^2}\left(\frac{1}{C_b + C_w}\right) + \left(\frac{1}{s + Z_2}\right) \cdot \right. \\ & \left. \left(\frac{Z_3(Z_1 - Z_2)}{Z_2[C_b(Z_2^2 - (Z_1 + Z_3)Z_2 + Z_1 Z_3(1 + C_w/C_b))]}\right) \right. \\ & + \left[\frac{r_1 \exp\{j\theta_2\}}{(s + \alpha + \beta j)} + \frac{r_1 \exp\{-j\theta_2\}}{(s + \alpha - \beta j)}\right] P_h \\ & + \left[\frac{r_2 \exp\{j\theta_2\}}{(s + \alpha + \beta j)} + \frac{r_2 \exp\{-j\theta_2\}}{(s + \alpha - \beta j)}\right] T_w(0) \end{aligned} \tag{23}$$

The inverse transform of eqn (23) is

$$T_b(t) = \frac{P_h t}{(C_b + C_w)} + \frac{P_h Z_3(Z_1 - Z_2)\exp\{-Z_2 t\}}{Z_2[(Z_2^2 - Z_2(Z_1 + Z_3))C_b + Z_1 Z_3(C_b + C_w)]}$$

$$+ P_b r_1[\exp\{j\theta_1\}\exp\{-(\alpha + \beta j)t\}$$

$$+ \exp\{-j\theta_1\}\exp\{-(\alpha - \beta j)t\}]$$

$$+ \left[T_b(0) + \tau_w \left(\frac{dT_b}{dt}\right)_{t=0}\right] [r_2(\exp\{j\theta_2\}\exp\{-(\alpha + \beta j)t\}$$

$$+ \exp\{-j\theta_2\}\exp\{-(\alpha + \beta j)t\})] \tag{24}$$

The value dT_b/dt at $t = 0$ in eqn (24) is the background heating rate, γ_{bkg}.

Evaluating the exponential terms in j,

$$T_b(t) = P_b \left[\frac{t}{(C_b + C_w)} + \frac{Z_3(Z_1 - Z_2)\exp\{-Z_2 t\}}{Z_2[(Z_2^2 - Z_2(Z_1 + Z_3))C_b + Z_1 Z_3(C_b + C_w)]}\right.$$

$$\left. + 2r_1\exp\{-\alpha t\}\cos\{\beta t - \theta_1\}\right]$$

$$+ \frac{2\gamma_{bkg} r_2 \exp\{-\alpha t\}\cos\{\beta t - \theta_2\}}{Z_1} \tag{25}$$

Case II: The condition for critical damping is

$$\left(\frac{Z_1 + Z_3}{2}\right)^2 = Z_1 Z_3(1 + C_w/C_b) \tag{26}$$

and a single root for s in the second-order differential equation is obtained. Equation (11) can be written

$$T_b(s) = \frac{Z_2 Z_3}{C_b}\left[\frac{(s + Z_1)}{s^2(s + Z_2)(s + \alpha)^2}\right] P_b$$

$$+ \frac{Z_1 Z_3 C_w}{C_b}\left[\frac{1}{s(s + \alpha)^2}\right] T_w(0) \tag{27}$$

The coefficient of P_b in eqn (11) is factored as

$$\frac{K_8}{s^2} + \frac{K_9}{s + Z_2} + \frac{K_{10}}{(s + \alpha)^2} + \frac{K_{11}}{(s + \alpha)} \tag{28}$$

where

$$K_8 = \frac{Z_1 Z_3}{C_b \alpha^2} \tag{29}$$

$$K_9 = \frac{Z_3(Z_2 - Z_1)}{C_b Z_2(\alpha - Z_2)^2} \tag{30}$$

$$K_{10} = \frac{Z_2 Z_3(Z_1 - \alpha)}{C_b \alpha^2 (Z_2 - \alpha)} \tag{31}$$

$$K_{11} = \frac{Z_2 Z_3}{C_b}\left[\frac{\alpha^2(Z_2 - \alpha) - (Z_1 - \alpha)(3\alpha^2 - 2\alpha Z_2)}{\alpha^4 (Z_2 - \alpha)^2}\right] \tag{32}$$

The coefficient of $T_w(0)$ in eqn (11) is factored as

$$\frac{K_{12}}{s} + \frac{K_{13}}{(s+\alpha)^2} + \frac{K_{14}}{(s+\alpha)} \tag{33}$$

where

$$K_{12} = \frac{Z_1 Z_3 C_w}{\alpha^2 C_b} \tag{34}$$

$$K_{13} = \frac{-Z_1 Z_3 C_w}{\alpha C_b} \tag{35}$$

$$K_{14} = \frac{-Z_1 Z_3 C_w}{\alpha^2 C_b} \tag{36}$$

The inverse transform of eqn (11) for the critically damped system is

$$\begin{aligned} T_b(t) = {} & \frac{P_h}{C_b}\left[\frac{Z_1 Z_3 t}{\alpha^2} + \frac{Z_3(Z_2 - Z_1)\exp\{-Z_2 t\}}{Z_2(\alpha - Z_2)^2}\right. \\ & \left. + \frac{Z_2 Z_3 (Z_1 - \alpha) t \exp\{-\alpha t\}}{\alpha^2 (Z_2 - \alpha)}\right] \\ & + \frac{\gamma_{bkz}}{C_b}\left[\frac{Z_3 C_w}{\alpha^2} - \frac{Z_3 C_w t \exp\{-\alpha t\}}{\alpha} - \frac{Z_3 C_w \exp\{-\alpha t\}}{\alpha^2}\right] \end{aligned} \tag{37}$$

Case III: The case of an overdamped system occurs when

$$\left(\frac{Z_1 + Z_3}{2}\right)^2 > Z_1 Z_3 (1 + C_w / C_b) \tag{38}$$

The coefficient of P_h is factored as

$$\frac{K_{15}}{s^2} + \frac{K_{16}}{(s + Z_2)} + \frac{K_{17}}{(s + \alpha + \sigma)} + \frac{K_{18}}{(s + \alpha - \sigma)} \tag{39}$$

The constants are evaluated

$$K_{15} = \frac{Z_1Z_3}{C_b(\alpha + \sigma)(\alpha - \sigma)} \tag{40}$$

$$K_{16} = \frac{Z_3(Z_1 - Z_2)}{C_bZ_2(\alpha + \sigma - Z_2)(\alpha - \sigma - Z_2)} \tag{41}$$

$$K_{17} = \frac{-Z_2Z_3(Z_1 - \alpha - \sigma)}{2\sigma C_b(\alpha + \sigma)^2(Z_2 - \alpha - \sigma)} \tag{42}$$

$$K_{18} = \frac{Z_2Z_3(Z_1 - \alpha + \sigma)}{2C_b\sigma(\sigma - \alpha)^2(Z_2 - \alpha + \sigma)} \tag{43}$$

where

$$\sigma = \left[\left(\frac{Z_1 + Z_3}{2}\right)^2 - Z_1Z_3(1 + C_w/C_b)\right]^{1/2} \tag{44}$$

The coefficient of T_w (0) is factored

$$\frac{K_{19}}{s} + \frac{K_{20}}{(s + \alpha + \sigma)} + \frac{K_{21}}{(s + \alpha - \sigma)} \tag{44b}$$

where

$$K_{19} = \frac{Z_1Z_3C_w}{C_b(\alpha + \sigma)(\alpha - \sigma)} \tag{45}$$

$$K_{20} = \frac{Z_1Z_3C_w}{2\sigma C_b(\alpha - \sigma)} \tag{46}$$

$$K_{21} = \frac{Z_1Z_3C_w}{2\sigma C_b(\sigma - \alpha)} \tag{47}$$

The inverse transform of eqn (11) is

$$\begin{aligned} T_b(t) = {} & \frac{P_b}{C_b}\left[\frac{Z_1Z_3t}{(\alpha + \sigma)(\alpha - \sigma)} + \frac{Z_3(Z_1 - Z_2)\exp - Z_2t}{Z_2(\alpha + \sigma - Z_2)(\alpha - \sigma - Z_2)}\right. \\ & - \frac{Z_2Z_3(Z_1 - \alpha - \sigma)\exp\{-(\alpha + \sigma)t\}}{2\sigma(\alpha + \sigma)^2(Z_2 - \alpha - \sigma)} \\ & \left. + \frac{Z_2Z_3(Z_1 - \alpha + \sigma)\exp\{-(\alpha - \sigma)t\}}{2\sigma(\sigma - \alpha)^2(Z_2 - \alpha + \sigma)}\right] \\ & + \frac{\gamma_{bkz}}{C_b}\left[\frac{Z_3C_w}{(\alpha + \sigma)(\alpha - \sigma)} + \frac{Z_3C_w\exp\{-(\alpha + \sigma)t\}}{2\sigma(\alpha - \sigma)}\right. \\ & \left. + \frac{Z_3C_w\exp\{-(\alpha - \sigma)t\}}{2\sigma(\sigma - \alpha)}\right] \end{aligned} \tag{48}$$

Anterior period

The anterior period begins at the time in the main period for power cut off, $t = t_{co}$. Time at cut off is designated $t = 0$ for mathematical consideration of the anterior period. The general equation applies with the recognition that $dQ_h/dt = 0$ when $t > 0$

$$T_b(s) = \left[\frac{(s^2 + (Z_1 + Z_3)s + Z_1Z_3)}{s(s^2 + (Z_1 + Z_3)s + Z_1Z_3(1 + C_w/C_b))}\right] T_b(0)$$

$$+ \frac{C_wZ_1Z_3}{C_b}\left[\frac{1}{s(s^2 + (Z_1 + Z_3)s + Z_1Z_3(1 + C_w/C_b))}\right] T_w(0)$$

$$+ \left[\frac{(s + Z_1)}{s(s^2 + (Z_1 + Z_3)s + Z_1Z_3(1 + C_w/C_b))}\right] T'_b(0)$$

$$+ \frac{C_hZ_1Z_3}{C_b}\left[\frac{(s + Z_1)}{s(Z_2 + s)(s^2 + (Z_1 + Z_3)s + Z_1Z_3(1 + C_w/C_b))}\right] T_h(0) \qquad (49)$$

The denominator of each term contains the second-order differential equation considered above as a function of the system damping.

Case I: When the system is in an underdamped condition the coefficient of $T_h(0)$ can be written as

$$\frac{L_1}{s} + \frac{L_2}{s + Z_2} + \frac{L_3}{s + \alpha + \beta j} + \frac{L_4}{s + \alpha - \beta j} \qquad (50)$$

where

$$L_1 = \frac{C_h}{C_b + C_w} \qquad (51)$$

$$L_2 = \frac{C_hZ_3(Z_2 - Z_1)}{C_b(Z_2^2 - Z_2(Z_1 + Z_3) + Z_1Z_3(1 + C_w/C_b))} \qquad (52)$$

$$L_3 = \frac{-C_hr_1\exp\{j\theta_1\}}{C_b + C_w} \qquad (53)$$

$$L_4 = \frac{-C_hr_1\exp\{-j\theta_1\}}{C_b + C_w} \qquad (54)$$

and α, β, r_1 and θ_1 were defined previously.

The coefficient of the $T_b(0)$ term can be written as

$$\frac{L_5}{s} + \frac{L_6}{s + \alpha + \beta j} + \frac{L_7}{s + \alpha - \beta j} \qquad (55)$$

It can be shown that

$$L_5 = \frac{C_b}{C_b + C_w} \tag{56}$$

$$L_6 = r_3 \exp\{j\theta_3\} \tag{57}$$

$$L_7 = r_3 \exp\{-j\theta_3\} \tag{58}$$

$$r_3 = [(a_3)^2 + (b_3)^2]^{1/2} \tag{59}$$

where

$$a_3 = \frac{-C_b[Z_1Z_3 - \alpha^2 - \beta^2]}{2Z_1Z_3(C_b + C_w)}$$

$$b_3 = \frac{-C_b[2\alpha\beta^2 + \alpha^3 - \alpha\beta^2 - (\alpha^2 + \beta^2)(Z_1 + Z_3) + \alpha Z_1Z_3]}{2Z_1Z_3\beta(C_b + C_w)}$$

$$\theta_3 = \arcsin b_3/r_3$$

The coefficient of the $T_w(0)$ term can be written as

$$\frac{L_8}{s} + \frac{L_9}{s + \alpha + \beta j} + \frac{L_{10}}{s + \alpha - \beta j} \tag{60}$$

It can be shown that

$$L_8 = \frac{C_w}{C_b + C_w} \tag{61}$$

$$L_9 = r_4 \exp\{j\theta_4\} \tag{62}$$

$$L_{10} = r_4 \exp\{-j\theta_4\} \tag{63}$$

where

$$r_4 = [(a_4)^2 + (b_4)^2]^{1/2}$$

$$a_4 = \frac{-C_w}{2(C_b + C_w)}$$

$$b_4 = \frac{-\alpha C_w}{2(C_b + C_w)\beta}$$

$$\theta_4 = \arcsin\{b_4/r_4\}$$

The coefficient of the $T_b'(0)$ term can be written as

$$\frac{L_{11}}{s} + \frac{L_{12}}{s + \alpha + \beta j} + \frac{L_{13}}{s + \alpha - \beta j} \tag{64}$$

It can be shown that

$$L_{11} = \frac{C_b}{Z_3(C_b + C_w)} \tag{65}$$

$$L_{12} = -\, r_5 \exp\{j\theta_5\} \tag{66}$$

$$L_{13} = -\, r_5 \exp\{-\, j\theta_5\} \tag{67}$$

where

$$r_5 = [(a_5)^2 + (b_5)^2]^{1/2}$$

$$a_5 = \frac{C_b}{2Z_3(C_b + C_w)}$$

$$b_5 = \frac{C_b(\alpha Z_1 - \alpha^2 - \beta^2)}{2Z_1 Z_3 \beta (C_b + C_w)}$$

$$\theta_5 = \arcsin\{b_5/r_5\}$$

Equation (49) now becomes

$$\begin{aligned}
T_b(s) = &\left[\left(\frac{C_b}{C_b + C_w}\right)\left(\frac{1}{s}\right) + \frac{r_3\exp\{j\theta_3\}}{(s + \alpha + \beta j)} + \frac{r_3\exp\{-\, j\theta_3\}}{(s + \alpha - \beta j)}\right] T_b(0) \\
&+ \left[\left(\frac{C_w}{C_b + C_w}\right)\left(\frac{1}{s}\right) + \frac{r_4\exp\{j\theta_4\}}{(s + \alpha + \beta j)} + \frac{r_4\exp\{-\, j\theta_4\}}{(s + \alpha - \beta j)}\right] T_w(0) \\
&+ \left[\left(\frac{C_b}{Z_3(C_b + C_w)}\right)\left(\frac{1}{s}\right) - \frac{r_5\exp\{j\theta_5\}}{(s + \alpha + \beta j)} - \frac{r_5\exp\{-\, j\theta_5\}}{(s + \alpha - \beta j)}\right] T_b'(0) \\
&+ \left[\left(\frac{C_h}{C_b + C_w}\right)\left(\frac{1}{s}\right) - \frac{C_h Z_3(Z_1 - Z_2)}{C_b(Z_2^2 - Z_2(Z_1 + Z_3) + Z_1 Z_3(1 + C_w/C_b))(s + Z_2)}\right. \\
&\left. - \frac{C_h r_2\exp\{j\theta_2\}}{(C_b + C_w)(s + \alpha + \beta j)} - \frac{C_h r_2\exp\{-\, j\theta_2\}}{(C_b + C_w)(s + \alpha - \beta j)}\right] T_h(0)
\end{aligned} \tag{68}$$

The initial conditions for the anterior period correspond to the conditions at $t = t_{co}$ for the main period. Provided the main period is of sufficient length the heater is at a steady-state temperature

$$\left(\frac{dT_h}{dt}\right)_{t=t_{co}} \simeq T_h'(0) \simeq 0$$

Hence from eqns (4) and (6)

$$T_h(0) = \frac{P_h}{h_h A_h} + T_{bf}(0) = \frac{P_h}{h_h A_h} + \frac{P_h t_{co}}{C_b + C_w} + \tau_m \gamma_b$$

The value of $T_b(0)$ for the anterior period is determined by P_h, t_{co}, and the heat capacity terms, C_b and C_w

$$T_b(0) = \frac{P_h t_{co}}{C_b + C_w} \tag{69}$$

It follows that

$$T_b'(0) = \frac{P_h}{C_b + C_w} \tag{70}$$

Inequality of $T_w'(0)$ and $T_b'(0)$ must be accounted for because at $t = t_{co}$, $T_w(0) \neq T_b(0)$. The background correction term is called γ_{bkg} and

$$\frac{dT_w(0)}{dt} = \frac{dT_b(0)}{dt} - \gamma_{bkg}$$

$$= \frac{P_h}{C_b + C_w} - \gamma_{bkg} \tag{71}$$

From eqn (2)

$$\frac{1}{Z_1}\left(\frac{dT_w(0)}{dt}\right) = T_b(0) - T_w(0) \tag{72}$$

and

$$T_w(0) = T_b(0) - \frac{1}{Z_1}\left(\frac{dT_w(0)}{dt}\right)$$

$$= \frac{P_h t_{co}}{C_b + C_w} - \frac{1}{Z_1}\left(\frac{P_h}{C_b + C_w} - \gamma_{bkg}\right) \tag{73}$$

The inverse transform of eqn (68) is

$$T_b(t) = \left[\left(\frac{C_b}{C_b + C_w}\right) + 2r_3\exp\{-\alpha t\}\cos\{\beta t - \theta_3\}\right]\left[\frac{P_h t_{co}}{C_b + C_w}\right] \tag{74}$$

$$+ \left[\left(\frac{C_w}{C_b + C_b}\right) + 2r_4\exp\{-\alpha t\}\cos\{\beta t - \theta_4\}\right]\left[\frac{P_h t_{co}}{C_b + C_w}\right.$$

$$\left. - \frac{P_h}{Z(_1C_b + C_w)} + \frac{\gamma_{bkg}}{Z_1}\right]$$

$$+ \left[\frac{C_b}{Z_3(C_b + C_w)} - 2r_5 \exp\{-\alpha t\} \cos\{\beta t - \theta_5\}\right] \left[\frac{P_h}{C_b + C_w}\right]$$

$$+ \left[\left(\frac{C_h}{C_b + C_w}\right) + \frac{C_h Z_3(Z_2 - Z_1)\exp\{-Z_2 t\}}{C_b(Z_2^2 - Z_2(Z_1 + Z_3) + Z_1 Z_3(1 + C_w/C_b))}\right.$$

$$\left. - \frac{2C_h r_2 \exp\{-\alpha t\} \cos\{\beta t - \theta_2\}}{(C_b + C_w)}\right] \left[\frac{P_h}{h_h A_h} + \frac{P_h t_{co}}{C_b + C_w} + \tau_m \gamma_b\right] \tag{74}$$

Case II: For critical system damping,

$$\left(\frac{Z_1 + Z_3}{2}\right)^2 = Z_1 Z_3(1 + C_w/C_b) \tag{75}$$

and eqn (49) is written

$$T_b(s) = \left[\frac{(s + Z_1)(s + Z_3)}{s(s + \alpha)^2}\right] T_n(0)$$

$$+ \frac{Z_1 Z_3 C_w}{C_b} \left[\frac{1}{s(s + \alpha)^2}\right] T_w(0) \tag{76}$$

$$+ \left[\frac{(s + Z_1)}{s(s + \alpha)^2}\right] T_b'(0) + \frac{Z_2 Z_3 C_h}{C_b} \left[\frac{(s + Z_1)}{s(s + Z_2)(s + \alpha)^2}\right] T_h(0)$$

The coefficient of $T_h(0)$ can be factored as

$$\frac{L_{14}}{s} + \frac{L_{15}}{s + Z_2} + \frac{L_{16}}{(s + \alpha)^2} + \frac{L_{17}}{s + \alpha} \tag{77}$$

where

$$L_{14} = \frac{Z_1 Z_3 C_h}{\alpha^2 C_b} \tag{78}$$

$$L_{15} = \frac{Z_3(Z_2 - Z_1)C_h}{(\alpha - Z_2)^2 C_b} \tag{79}$$

$$L_{16} = \frac{Z_2 Z_3(Z_1 - \alpha)C_h}{\alpha(\alpha - Z_2)C_b} \tag{80}$$

$$L_{17} = \frac{Z_2 Z_3 C_h}{C_b} \left[\frac{\alpha(\alpha - Z_2) - (Z_1 - \alpha)(Z_2 - 2\alpha)}{\alpha^2(Z_2 - \alpha)^2}\right] \tag{81}$$

The coefficient of $T_b(0)$ can be written as

$$\frac{L_{18}}{s} + \frac{L_{19}}{(s+\alpha)^2} + \frac{L_{20}}{(s+\alpha)} \tag{82}$$

where

$$L_{18} = \frac{Z_1 Z_3}{\alpha^3} \tag{83}$$

$$L_{19} = \frac{-(Z_1-\alpha)(Z_3-\alpha)}{\alpha} \tag{84}$$

$$L_{20} = \frac{\alpha(Z_1 + Z_3 - 2\alpha) - (Z_1-\alpha)(Z_3-\alpha)}{\alpha^2} \tag{85}$$

The coefficient of the $T_b'(0)$ term can be written

$$\frac{L_{21}}{s} + \frac{L_{22}}{(s+\alpha)^2} + \frac{L_{23}}{(s+\alpha)} \tag{86}$$

where

$$L_{21} = \frac{Z_1}{\alpha^2} \tag{87}$$

$$L_{22} = \frac{(\alpha - Z_1)}{\alpha} \tag{88}$$

$$L_{23} = \frac{-Z_1}{\alpha^2} \tag{89}$$

The coefficient of $T_w(0)$ can be written

$$\frac{L_{24}}{s} + \frac{L_{25}}{(s+\alpha)^2} + \frac{L_{26}}{(s+\alpha)} \tag{90}$$

where

$$L_{24} = \frac{Z_1 Z_3 C_w}{\alpha^2 C_b} \tag{91}$$

$$L_{25} = \frac{-Z_1 Z_3 C_w}{\alpha\, C_b} \tag{92}$$

$$L_{26} = \frac{Z_1 Z_3 C_w}{\alpha^2 C_b} \tag{93}$$

Equation (49) can now be written

$$T_b(s) = + \left[\frac{\alpha[Z_1 + Z_3 - 2\alpha] - (Z_1 - \alpha)(Z_3 - \alpha)}{\alpha^2(s + \alpha)}\right] T_b(0)$$

$$+ \left[\frac{Z_1Z_3C_w}{\alpha^2C_bs} - \frac{Z_1Z_3C_w}{\alpha\, C_b(s + \alpha)^2} + \frac{Z_1Z_3C_w}{\alpha^2C_b(s + \alpha)}\right] T_w(0)$$

$$+ \left[\frac{Z_1}{\alpha^2s} + \frac{(\alpha - Z_1)}{\alpha(s + \alpha)^2} - \frac{Z_1}{\alpha^2(s + \alpha)}\right] T_b'(0)$$

$$+ \left[\frac{Z_1Z_3C_h}{\alpha^2C_bs} + \frac{Z_3(Z_2 - Z_1)C_h}{(\alpha - Z_2)^2C_b(s + Z_2)} + \frac{Z_2Z_3(Z_1 - \alpha)C_h}{\alpha(\alpha - Z_2)C_b(s + \alpha)^2}\right.$$

$$\left. + \frac{C_hZ_2Z_3}{C_b(s + \alpha)}\left(\frac{\alpha(\alpha - Z_2) - (Z_1 - \alpha)(Z_2 - 2\alpha)}{\alpha^2(Z_2 - \alpha)^2}\right)\right] T_h(0) \tag{94}$$

Taking the inverse transform of eqn (94)

$$T_b(t) = \left[\frac{Z_1Z_3}{\alpha^2} - \frac{(Z_1 - \alpha)(Z_3 - \alpha)t\exp\{-\alpha t\}}{\alpha}\right.$$

$$\left. + \left(\frac{\alpha(Z_1 + Z_3 - 2\alpha) - (Z_1 - \alpha)(Z_3 - \alpha)}{\alpha^2}\right)\exp\{-\alpha t\}\right] \cdot$$

$$\left[\frac{P_ht_{co}}{C_b + C_w}\right] + \left[\frac{Z_1Z_3C_w}{\alpha^2C_b} - \frac{Z_1Z_3tC_w\exp\{-\alpha t\}}{\alpha C_b}\right.$$

$$\left. + \frac{Z_1Z_3C_w\exp\{-\alpha t\}}{\alpha^2C_b}\right]\left[\frac{P_ht_{co}}{C_b + C_w} - \frac{P_h}{Z_1(C_b + C_w)} + \frac{\gamma_{bkg}}{Z_1}\right]$$

$$+ \left[\frac{Z_1}{\alpha^2} + \frac{(\alpha - Z_1)t\exp\{-\alpha t\}}{\alpha} - \frac{Z_1\exp\{-\alpha t\}}{\alpha^2}\right]\left[\frac{P_h}{C_b + C_w}\right]$$

$$+ \left[\frac{Z_1Z_3C_h}{\alpha^2C_b} + \frac{Z_3(Z_2 - Z_1)C_h\exp\{-Z_2t\}}{(\alpha - Z_2)^2C_b}\right.$$

$$+ \frac{Z_2Z_3(Z_1 - \alpha)C_ht\exp\{-\alpha t\}}{\alpha(\alpha - Z_2)C_b} + C_hZ_2Z_3 \cdot$$

$$\left.\left(\frac{(\alpha^2 - \alpha Z_2) - (Z_1 - \alpha)(Z_2 - 2\alpha)}{\alpha^2(Z_2 - \alpha)^2C_b}\right)\exp\{-\alpha t\}\right] \cdot$$

$$\left[\frac{P_h}{h_h A_h} + \frac{P_h t_{co}}{C_b + C_w} \tau_m \gamma_b\right] \tag{95}$$

Case III: For the case of over damping the coefficient of $T_h(0)$ can be written

$$\frac{L_{27}}{s} + \frac{L_{28}}{(s + Z_2)} + \frac{L_{29}}{(s + \alpha + \sigma)} + \frac{L_{30}}{(s + \alpha - \sigma)} \tag{96}$$

where

$$L_{27} = \frac{Z_1 Z_3 C_h}{(\alpha + \sigma)(\alpha - \sigma) C_b} \tag{97}$$

$$L_{28} = \frac{Z_3 (Z_2 - Z_1) C_h}{(\alpha + \sigma - Z_2)(\alpha - \sigma - Z_2) C_b} \tag{98}$$

$$L_{29} = \frac{C_h Z_2 Z_3 (Z_1 - \alpha - \sigma)}{C_b 2\sigma (\alpha + \sigma)(Z_2 - \alpha - \sigma)} \tag{99}$$

$$L_{30} = \frac{- C_h Z_2 Z_3 (Z_1 - \alpha + \sigma)}{2 C_b \sigma (\alpha - \sigma)(Z_2 - \alpha + \sigma)} \tag{100}$$

The coefficient of $T_b(0)$ can be written as

$$\frac{L_{31}}{s} + \frac{L_{32}}{(s + \alpha + \sigma)} + \frac{L_{33}}{(s + \alpha - \sigma)} \tag{101}$$

where

$$L_{31} = \frac{Z_1 Z_3}{(\alpha + \sigma)(\alpha - \sigma)} \tag{102}$$

$$L_{32} = \frac{(Z_1 - \alpha - \sigma)(Z_3 - \alpha - \sigma)}{2\sigma(\alpha + \sigma)} \tag{103}$$

$$L_{33} = \frac{(Z_1 - \alpha + \sigma)(Z_3 - \alpha + \sigma)}{2\sigma(\sigma - \alpha)} \tag{104}$$

The coefficient of $T_b(0)$ can be written

$$\frac{L_{34}}{s} + \frac{L_{35}}{(s + \alpha + \sigma)} + \frac{L_{36}}{(s + \alpha - \sigma)} \tag{105}$$

where

$$L_{34} = \frac{Z_1}{(\alpha + \sigma)(\alpha - \sigma)} \tag{106}$$

$$L_{35} = \frac{Z_1 - \alpha - \sigma}{2\sigma(\alpha + \sigma)} \tag{107}$$

$$L_{36} = \frac{Z_1 - \alpha + \sigma}{2\sigma(\sigma - \alpha)} \tag{108}$$

The coefficient of $T_w(0)$ can be written

$$\frac{L_{37}}{s} + \frac{L_{38}}{(s + \alpha + \sigma)} + \frac{L_{39}}{(s + \alpha - \sigma)} \tag{109}$$

where

$$L_{37} = \frac{Z_1 Z_3 C_w}{(\alpha + \sigma)(\alpha - \sigma)C_b} \tag{110}$$

$$L_{38} = \frac{Z_1 Z_3 C_w}{2\sigma(\alpha + \sigma)C_b} \tag{111}$$

$$L_{39} = \frac{Z_1 Z_3 C_w}{2\sigma(\sigma - \alpha)C_b} \tag{112}$$

Equation (49) is now written

$$\begin{aligned}
T_b(s) = {} & \left[\frac{Z_1 Z_3}{s(\alpha + \sigma)(\alpha - \sigma)} + \frac{(Z_1 - \alpha - \sigma)(Z_3 - \alpha - \sigma)}{2\sigma(\alpha + \sigma)(s + \alpha + \sigma)}\right. \\
& \left. + \frac{(Z_1 - \alpha + \sigma)(Z_3 - \alpha + \sigma)}{2\sigma(\sigma - \alpha)(s + \alpha - \sigma)}\right] T_b(0) \\
& + \left[\frac{Z_1 Z_3 C_w}{s(\alpha + \sigma)(\alpha - \sigma)C_b} + \frac{Z_1 Z_3 C_w}{2\sigma C_b(\alpha + \sigma)(s + \alpha + \sigma)}\right. \\
& \left. + \frac{Z_1 Z_3 C_w}{2\sigma C_b(\sigma - \alpha)(s + \alpha - \sigma)}\right] T_w(0) \\
& + \left[\frac{Z_1}{s(\alpha + \sigma)(\alpha - \sigma)} + \frac{Z_1 - \alpha - \sigma}{2\sigma(\alpha + \sigma)(s + \alpha + \sigma)}\right. \\
& \left. + \frac{Z_1 - \alpha + \sigma}{2\sigma(\sigma - \alpha)(s + \alpha - \sigma)}\right] T_b'(0) + \left[\frac{Z_1 Z_3 C_b}{s(\alpha + \sigma)(\alpha - \sigma)C_b}\right. \\
& + \frac{C_b Z_3(Z_2 - Z_1)}{C_b(\alpha + \sigma - Z_2)(\alpha - \sigma - Z_2)(s + Z_2)}
\end{aligned}$$

$$+\frac{C_b Z_2 Z_3(Z_1-\alpha-\sigma)}{2C_b\sigma(\alpha+\sigma)(Z_2-\alpha-\sigma)(s+\alpha+\sigma)}$$

$$-\left.\frac{C_b Z_2 Z_3(Z_1-\alpha+\sigma)}{2C_b\sigma(\alpha-\sigma)(Z_2-\alpha+\sigma)(s+\alpha-\sigma)}\right] T_b(0) \tag{113}$$

The inverse transform of Eqn (113) is

$$T_b(t)=\left[\frac{Z_1Z_3}{(\alpha+\sigma)(\alpha-\sigma)}+\frac{(Z_1-\alpha-\sigma)(Z_3-\alpha-\sigma)\exp\{-(\alpha+\sigma)t\}}{2\sigma(\alpha+\sigma)}\right.$$

$$\left.+\frac{(Z_1-\alpha+\sigma)(Z_3-\alpha+\sigma)\exp\{-(\alpha-\sigma)t\}}{2\sigma(\sigma-\alpha)}\right]\left[\frac{P_h t_{co}}{C_b+C_w}\right]$$

$$+\left[\frac{Z_1Z_3C_b}{(\alpha+\sigma)(\alpha-\sigma)C_b}+\frac{Z_3(Z_2-Z_1)\,C_b\exp\{-Z_2t\}}{(\alpha+\sigma-Z_2)(\alpha-\sigma-Z_2)C_b}\right.$$

$$+\frac{Z_2Z_3(Z_1-\alpha-\sigma)C_b\exp\{-(\alpha+\sigma)t\}}{2\sigma(\alpha+\sigma)(Z_2-\alpha-\sigma)C_b}$$

$$\left.-\frac{Z_2Z_3(Z_1-\alpha+\sigma)C_b\exp\{-(\alpha-\sigma)t\}}{2\sigma(\alpha-\sigma)(Z_2-\alpha+\sigma)C_b}\right]\left[\frac{P_h}{h_bA_b}\right.$$

$$\left.+\frac{P_h t_{co}}{C_b+C_w}\tau_m\gamma_b\right]+\left[\frac{Z_1Z_3C_w}{(\alpha+\sigma)(\alpha-\sigma)C_b}\right.$$

$$\left.+\frac{Z_1Z_3C_w\exp\{-(\alpha+\sigma)t\}}{2\sigma(\alpha+\sigma)C_b}+\frac{Z_1Z_3C_w\exp\{-(\alpha-\sigma)t\}}{2\sigma(\sigma-\alpha)C_b}\right]\cdot$$

$$\left[\frac{P_h t_{co}}{C_b+C_w}-\frac{P_h}{Z_1(C_b+C_w)}+\frac{\gamma_{bkg}}{Z_1}\right]$$

$$+\left[\frac{Z_1}{(\alpha+\sigma)(\alpha-\sigma)}+\frac{(Z_1-\alpha-\sigma)\exp\{-(\alpha+\sigma)t\}}{2\sigma(\alpha+\sigma)}\right.$$

$$\left.+\frac{(Z_1-\alpha+\sigma)\exp\{-(\alpha-\sigma)t\}}{2\sigma(\sigma-\alpha)}\right]\left[\frac{P_h}{C_b+C_w}\right] \tag{114}$$

Implementation of calculations

Values of the time constants τ_b, τ_w, and τ_m must be accurately computed to account for the various mechanisms of heat conduction and convection occurring at the heater, disc stirrer, and cell wall. The geometry of the heater is cylindrical with a hemispherical tip. Terms in preceding equations for τ_h

$$Z_2 = 1/\tau_h = h_h A_h / C_h$$

which do not account for differing rates of heat transport over the surface of the heater are replaced by

$$Z_2 = \frac{h_h A_h}{C_h}\left[\frac{\lambda_h}{h_{hs} r_h}\right] \tag{115}$$

The value of h_{hs} is calculated by the equation of Scadron and Warshawsky[12] given below.

$$h_{hs} = 0.239\left[\left(\frac{U(r)}{U_{max}}\right)\frac{\omega_s r_s 2r_h}{v_b}\right]^{0.50}\left[\frac{v_b c_b}{\lambda_b}\right]^{0.30}\left[\frac{\lambda_b}{r_h}\right] \tag{116}$$

The value of C_h was calculated assuming the metal-film resistor to be[13] essentially Al_2O_3. Thus,

$$C_h = m_r c_r + m_{Cu} c_{Cu}$$

The equivalent thermal conductivity of the electrical heater is given by

$$\lambda_h = \lambda_r \frac{\lambda_{Cu}\lambda_e}{\lambda_{Cu}\lambda_e + x_{Cu}/r_h\lambda_e\lambda_r + x_{e,h}/r_h\lambda_{Cu}\lambda_r}$$

Heat gain by stem conduction of the probes is computed with the conduction of the cell wall

$$\tau_w = C_w(1/h_w A_w + 1/h_{stem}A_{stem})$$

All solution probes are considered to be of equal size and composition and to be positioned at identical distances from the center of the cell. The calculation of h_{stem} must account for stirring effects of the rotating shaft and the disc of the stirrer. This is done by using weighting factors

$$h_{stem} = \left[\frac{r_{sh}}{r_{sh} + r_s}\right]^{2/3} h_{stem,\,shaft} + \left[\frac{r_s}{r_{sh} + r_s}\right]^{2/3} h_{stem,disc}$$

The values of $h_{stem,\,shaft}$ and $h_{stem,\,disc}$ are calculated by the equation of Žukauskas[14] given here for $h_{stem,\,shaft}$.

$$h_{stem,shaft} = 0.135\left[\left(\frac{U(r)}{U_{max}}\right)\frac{\omega_s r_{sh} 2r_{stem}}{v_b}\right]^{0.63}\left[\frac{v_b c_b}{\lambda_b}\right]^{0.36}\left[\frac{\lambda_b}{r_{stem}}\right] \tag{117}$$

Equation (117) is particularly suited for cylinders with diameters greater than 0.25 in, whereas the equation of Scadron and Warshawsky[12] is applicable to cylinders of smaller diameter. The value of h_w is calculated from the equation of Nagata et al.[15] for an unbaffled vessel containing a cooling coil

$$h_w = 0.128\left[\frac{0.637 r_s^2 \omega_s}{v_b}\right]^{0.667}\left[\frac{v_b c_b}{\lambda_b}\right]^{0.33}\left[\frac{r_s}{r_c}\right]^{-0.25}\left[\frac{l_1}{l_2}\right]^{0.15}.$$

$$\left[\frac{x_s}{2r_c}\right]^{0.15}\left[\frac{\lambda_b l_2}{r_c^2}\right] \tag{118}$$

Efficient solution mixing in the cell results from uniform turbulent flow. The time constant of mixing, τ_m, used for derivations described here was defined specifically in terms of the rate of heat transport across the thermal boundary layer of the heater (see eqn (6)). The surface of the rotating disc and, to a lesser extent, the surface of the shaft provide the stirring. Stirring by the disc results when fluid is pumped from the fluid bulk in an axial direction to the surface of the disc from whence it flows radially over the surfaces of the probes. Stirring by the shaft also results from radial and angular fluid flow. The net value of τ_m is taken to be the harmonic mean of individual time constants computed for stirring by the disc and by the shaft.

$$\tau_m = \left[\frac{1/\tau_{m,\mathrm{disc}} + 1/\tau_{m,\mathrm{shaft}}}{2}\right]^{-1}$$

The values of $\tau_{m,\,\mathrm{disc}}$ and $\tau_{m,\,\mathrm{shaft}}$ were calculated from the fluid velocity at the position of the heater by application of equations derived for turbulent mixing in pipe flow described by Brodkey[10]. The choice of analogy between mixing at the heater and that for pipe flow was made of necessity since rigorous treatment of turbulent mixing to our knowledge has been accomplished only for pipe flow. The radial fluid velocity at the rim of the disc is corrected by the Pai power series to give the velocity at the position of the electrical heater. The radical assumption is then made that this velocity is analogous to the mainstream velocity of the pipe flow treated by Brodkey. The value of τ_m weakly reflects variation of the Schmidt number. Although the Schmidt number for 0.01 M electrolyte solutions is more than 3 × that for water (1000 vs. 300), τ_m differs by only about 10%.

A spatial temperature function was derived to describe inhomogeneities of the bulk solution temperature which were disregarded in our initial discussion. The electrical heater is sufficiently small compared to the total volume of the calorimeter to be considered a point source of heat. Depending on the location of the temperature sensor relative to the electrical heater, the temperature sensor may be in a region of "excess" or "deficient" temperature. Considering ε to be the angle between the center point of the electrical heater and the longitudinal axis of the calorimeter and χ to be the angle between the electrical heater and the temperature sensor, it can be shown that there is a temperature difference function of the following form.

$$T_{b,t} - T_{b,\mathrm{ave}} = 3.14\,\gamma_{b,\mathrm{ave}}\,t\left(\frac{l_2}{r_c}\right)\left(\frac{\tau_m}{\tau_h}\right)\cos(\sigma_s\chi)\sin(\sigma_s\varepsilon)$$

where l_2/r_c is considered to be the cell asymmetry factor and σ_s the shielding parameter which describes the shielding of the temperature sensor by the stirrer and is given by

$$\sigma_s = \frac{U_s(r)}{U_{sh}(r)}\left[\frac{r_s^{2/3}}{(rr_c)^{1/3}}\right]$$

EXPERIMENTAL

Apparatus

A photograph of a new compact isoperibol calorimeter of the submarine type with variable heat shields above and around the Dewar cells is shown in Fig. 1. A photograph of the calorimeter probes is shown in Fig. 2. The design avoids the disadvantage of leaky seals which commonly plague completely submerged calorimeters by utilizing a lid with its own system of enclosed chambers for circulation of a thermostated liquid. The temperature of the lid can be maintained at a value independent of the Dewar cells by use of a separate thermostatic bath and circulation pump. The cell is unique in that no gaskets, flanges, or other parts need to be reassembled each time the calorimeter is used. Instead, the calorimeter cells are raised or lowered on a laboratory jack and can be moved to one side to facilitate addition of solution by pipeting or removal by aspiration. All manipulations including cleaning are accomplished quickly with minimal chance for component damage.

Two Aladdin 10-oz Dewar flasks (No. 020A) are mounted in four 1-l polyethylene bottles by means of the rubber rings and plastic base plates supplied with the containers for use as replacement fillers for vacuum bottles. A 24-ft. coil of 0.25-in. copper tubing for circulation of thermostated fluid sits on a cork ring trimmed to fit the bottom of the polyethylene bottle. There is approximately 0.5-in. clearance on each side of the coil. The Dewar cells are held in place by Plexiglas rings which also enclose the top of the polyethylene bottles. Mineral oil is placed in the bottles as a medium for heat transfer between the Dewar cell and the copper tubing. Circulating thermostated water is provided by a Forma Temp Jr. bath and circulator (No. 2095-2)

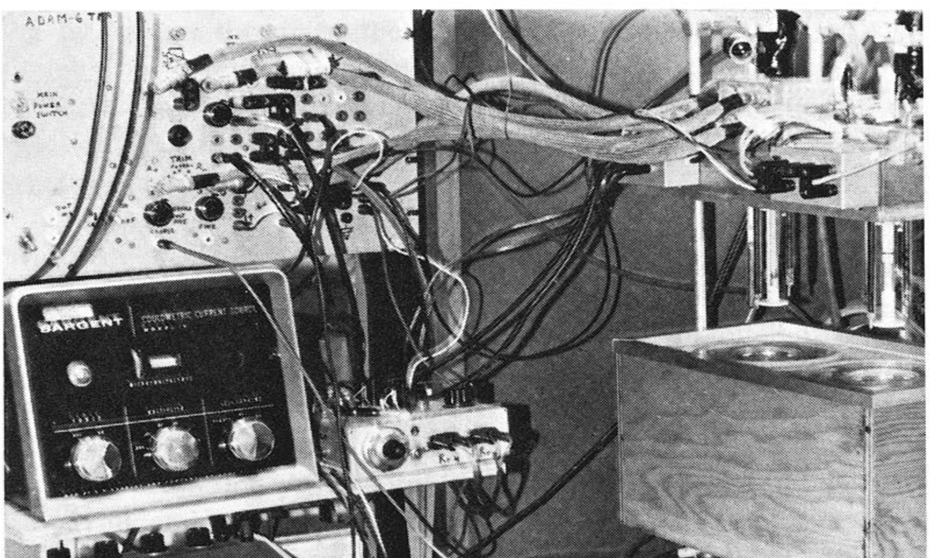

Fig. 1. Photograph of calorimeter.

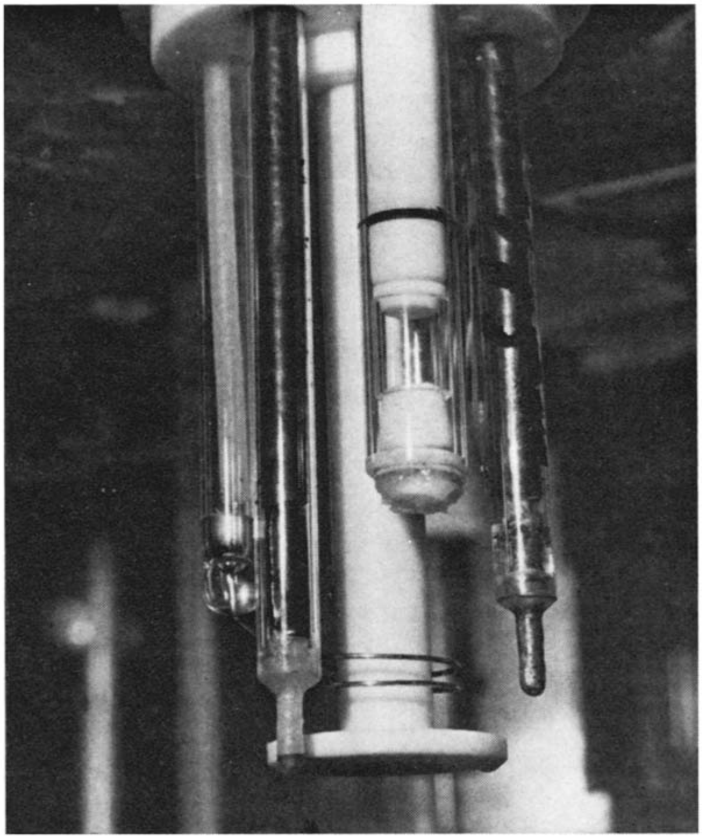

Fig. 2. Photograph of calorimeter probes.

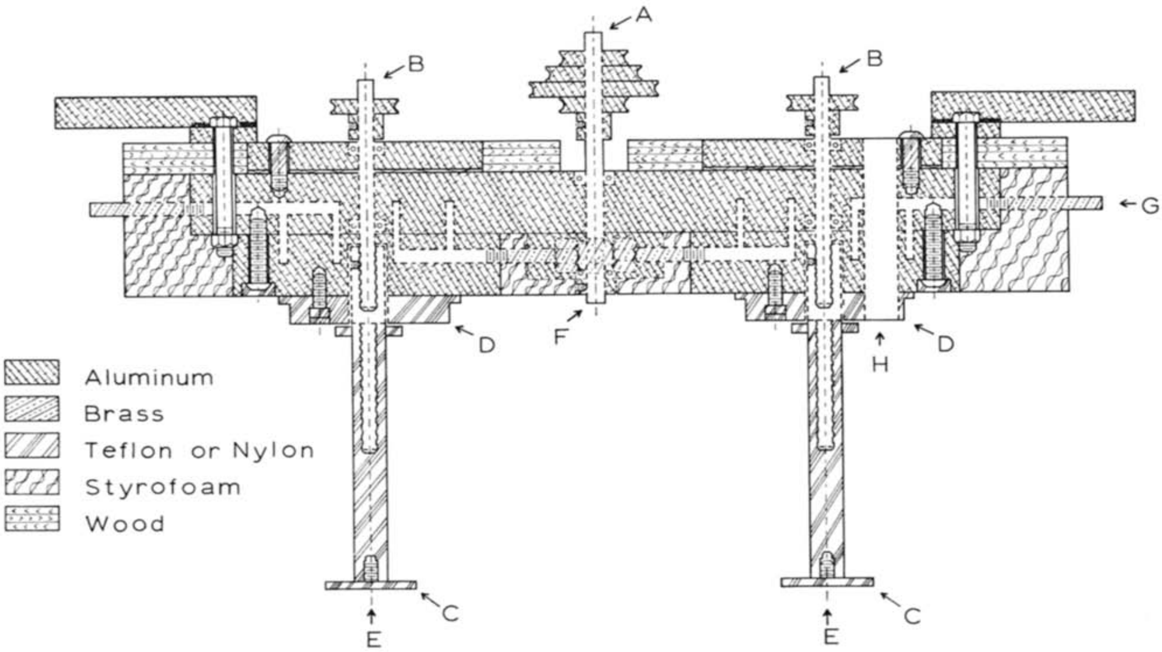

Fig. 3. Diagram of calorimeter head.

which provides temperature control to $\pm 0.02\,°C$. The temperature fluctuations of water from the Forma Temp Jr. were satisfactorily damped by passing the water through a 50-ft. coil of 0.38-in. polyethylene tubing placed in a 12-l mineral oil bath. The polyethylene bottles sit in laminated Styrofoam cases in a plywood box.

A detailed scale drawing of the calorimeter head is given in Fig. 3. A massive aluminum block with channels cut for the flow of thermostating fluid provides a large heat sink above and beyond the edges of the calorimeter cells. A thin coat of Dow Corning silicone rubber sealant is applied to prevent leakage when the large discs and main plate were bolted together. The tops of the calorimeter cells are ground flat so that a small amount of sealant grease applied to the Teflon cell covers provides a nearly vapor-tight seal. The calorimeter head is covered by a 1-in. thickness of Styrofoam on the sides and bottom. The top and sides of the head are covered additionally with plywood. The aluminum discs projecting below the block are covered with epoxy. Tygon tubing surrounds the four bolts used to connect the head and the mounting frame. When the calorimeter box is raised into position below the head, there are a series of interlocking seals made at the contact of the box and head.

Careful inspection of Fig. 3 reveals that the upper bearings of the calorimeter stirrers are mounted in aluminum blocks thermally separated from the main head block. The stirrers are driven by a single pulley with bearings mounted on the main head block and turned by a belt connected to a step pulley on a T-Line motor (No. 105) from Talboys Engineering Corp.

Titrant injection is made from 2.000-ml micrometer syringes driven by a variable-speed, reversible motor modified from the design as described by Ebell[16]. The flow-rates can be adjusted in the range 0–1 ml/min. An electrical braking mechanism allows exact shut-off at any point. Titrant solutions are brought to constant temperature by passage through a thermostated condenser tube. A 100-KΩ NTC thermistor mounted in the condenser jacket is used for monitoring of titrant temperature. The condensers are wrapped in glass wool and plastic tape for further thermal protection. Injection of titrant into the calorimeter cells is made through 6 mm OD $\times$ 0.5 mm ID pyrex capillaries tapered sharply at the point of injection.

Procedures

Since no method is described in the literature for selection of matched Dewar cells on the basis of thermal characteristics for use in differential calorimetry, a simple procedure was devised based on measurement of the cell heat-loss modulus. Each of ten Dewar flasks was filled with 250 ml of deionized water at ambient temperature (23–25 °C) and a Beckman thermometer centered in a No. 12 rubber stopper was placed in the water. After equilibration for 20–30 min, the Dewar was placed in a heated mineral-oil bath (39–41 °C). The temperature of the Dewar contents was measured at 1-min intervals for 30 min. The water was not stirred during the procedure. The heat-loss moduli for the cells were calculated from the heating curve by the method of Gunn[17].

The effect of stirring and the calorimeter head on the heating curve was determined as described above. A single Dewar flask was selected with $k = 1.2 \times 10^{-3}$ min^{-1}. The thermometer was inserted in the head through a port vacated by removal of a thermistor probe.

The overall heat-loss modulus of the reference cell for the assembled differential calorimeter was determined by two methods. Method A: The procedure of Swietoslawski[18] with temperature measurements made over a total time of 4.5×10^4 sec. Method B: The procedure of Gunn[17] as part of a determination of C_w.

Bulk solvents thermostated at 25.00 ± 0.02°C were pipetted using a specially designed 250-ml Pyrex pipet with a drain time of 90 sec. A total dispensing time of 100 sec was used for high precision in the volume delivered. The solvent used was triply distilled water boiled gently before delivery to a closed container and placement in the thermostatic bath. The order of solvent dispensing was as follows: the reference cell, two previously weighed polyethylene bottles, and the reaction cell. The polyethylene bottles were again weighed to determine the mass of water dispensed by the pipet. Typical uncertainties in the mass of solvent delivered are approximately ±0.014 g (95% confidence for 6 trials). All masses reported here are corrected to vacuum. The total time expired during solvent transfer was approximately 10 min.

Heat capacities of the calorimeter cells were determined by electrical heating with constant current from a Sargent Coulometric Current Source (Model IV). The current was calculated from the IR-drop across a standard resistor determined by a Leeds and Northrup K-2 potentiometer. Potentials across the resistance heaters were measured at the banana-jack connectors by the L & N K-2 potentiometer.

Energies were calculated in calories on the basis of the conversion factor 4.184 J cal^{-1}. The mechanical counter of the coulometer was used for all time measurements and was calibrated by comparison with the NBS radio time signals from Fort Collins, Colorado.

The time constant of mixing, τ_m, for the Dewar cells was estimated from photometric measurements made with a Pyrex cell matching closely the size and shape of the Dewar cell set in place of the reaction cell. A beam of blue light 1 cm in diameter was directed horizontally through the cell with the beam center 1.5 cm from the longitudinal axis of the cell. The cell contained 250 ml of water with 10 drops of 0.05% phenolphthalein. The output of a Heath 701A photomultiplier detector positioned to receive the transmitted light was recorded vs. time on a Sanborn oscillographic recorder as 0.25 ml of 50% NaOH solution was injected into the stirred solution. The transmittance of the solution was observed to decrease as an exponential function of time. The value of τ_m was taken as the point along the time axis when the change in transmittance was 0.632 of the total change.

The theoretical model for the response of the calorimeter bulk temperature, described above was programmed in WATFIV and executed on an IBM 360-5 digital computer in the Iowa State University Computation Center. A listing of the program is available on request from the authors. Further details are described in ref. 11.

RESULTS AND DISCUSSION

Heat-loss moduli

The heat-loss moduli, k, of ten Dewar cells were determined and the values are in the range 5.6×10^{-4} to 13.1×10^{-4} min^{-1}. Two cells matched within experimental error ($5.6 \pm 0.5 \times 10^{-4}$ min^{-1}) and were used in constructing the differential calorimeter.

The effect of the lid temperature, lid design, and the nature of bulk stirring on the measured heat loss modulus was studied with a single Dewar cell having $k = 1.2 \times 10^{-3}$ min^{-1}. Plots of temperature vs. time are shown in Fig. 4. The effect of a heated lid to change the value of k measured is substantial. The initial slope of the response curve for $T_{lid} = T_b + 16$°C was a factor of 1.51 greater than that for $T_{lid} = T_b$. This result is consistent with the conclusion of Sunner and Wadsö[4] that the design and temperature of the calorimeter lid affects the measured value of k. Their conclusion that the short term (<2 min) dynamic response is controlled by k is not correct. Our results described later show the short term response is primarily determined by mixing conditions. Long term (> 2 min) is greatly affected by k.

Data used for the computer simulation of e_o vs. t for the reference cell in the assembled calorimeter are given in Table 1 together with the results of calculations of k according to the methods of Swietslawski and Gunn. The agreement between

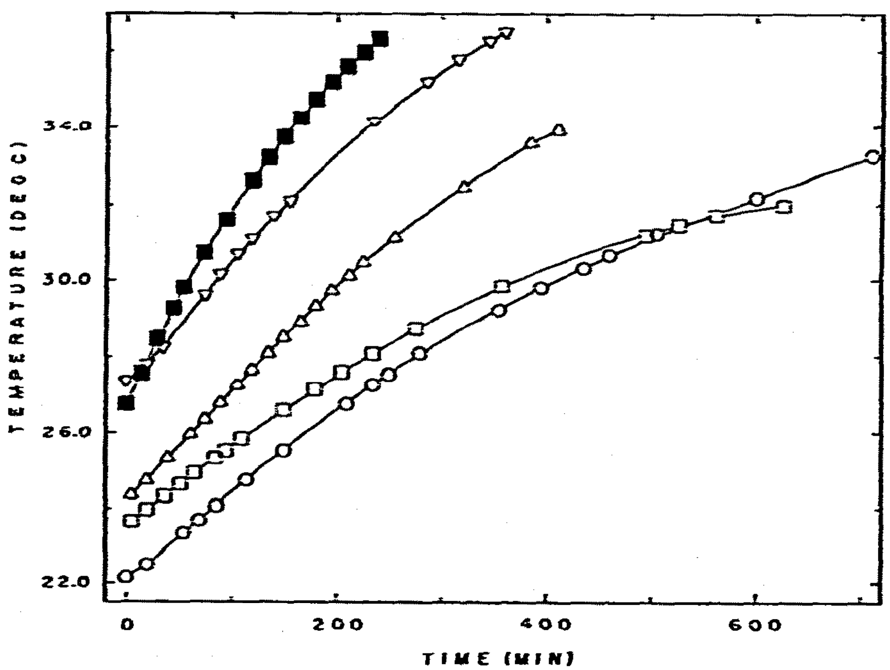

Fig. 4. Heat loss modulus of calorimeter dewar. $r_s = 1.63$ cm. ○ = rubber stopper, $N_s = 0$, ambient cell lid temperature; □ = Teflon stopper, $N_s = 0$, ambient cell lid temperature; △ = Teflon stopper, $N_s = 1760$ rev min^{-1}, ambient cell lid temperature; ■ = Teflon stopper, $N_s = 1760$ rev min^{-1}, cell lid heated to thermostat temperature; ▽ = Teflon stopper, $N_s = 0$, cell lid heated to thermostat temperature.

TABLE 1

PARAMETER VALUES FOR COMPUTER CALCULATIONS

Reference cell of calorimeter			
r_{sh}	= 0.64 cm	l_1	= 1.6 cm
r_c	= 2.96 cm	l_2	= 10.8 cm
r	= 2.15 cm	ε	= 0.7854 rad
r_{stem}	= 0.40 cm	χ	= 2.0246 rad
A_{stem}	= 181 cm^2	C_b	= 248.8 cal °C^{-1} (H_2O)
A_w	= 227 cm^2	C_w	= 33.3 cal °C^{-1}
x_s	= 0.35 cm	vapor volume	= 59.5 ml

Bulk solvent

Parameter	*Water, 25°C*	*Toluene, 25°C*
λ_b	1.45×10^{-3} cal cm^{-1} sec^{-1} °C^{-1} (ref. 20)	3.22×10^{-4} cal cm^{-1} sec^{-1} °C^{-1} (ref. 20)
ν_b	8.937×10^{-3} cm^2 sec^{-1}	6.42×10^{-3} cm^2 sec^{-1} (ref. 21)
Pr	6.16	7.11
Sc	297 (ref. 22)	257 (ref. 23)
c_p	0.998 cal g^{-1} °C^{-1} (ref. 21)	0.356 cal g^{-1} °C^{-1} (ref. 24)

Electrical

λ_h	3.9×10^{-3} cal cm^{-1} sec^{-1} °C^{-1}	A_h	= 1.2 cm^2
C_h	7×10^{-2} cal °C^{-1}	r_h	= 0.12 cm
γ_{bkg}	= 1.76×10^{-5} °C sec^{-1}	N_s	= 1000 rpm
		r_s	= 1.63 cm

Heat loss modulus of calorimeter cell

$k = 2.80 \times 10^{-3}$ min^{-1} (Method A)
$k = 2.87 \times 10^{-3}$ min^{-1} (Method B)

TABLE 2

THEORETICAL AND EXPERIMENTAL VALUES OF τ_m

Theoretical			*Experimental*		
N_s *(rpm)*	τ_m *(sec)*		N_s *(rpm)*	τ_m *(sec)*	
	$r = 1.55$ *cm*	$r = 2.15$ *cm*		$r = 1.5$ *cm*	
200	3.68	2.58	252	1.87	2.50
400	1.91	1.34	441	1.19	0.93
600	1.31	0.92	635	0.88	0.81
800	1.00	0.70	817	0.95	0.63
1000	0.81	0.57	1000	0.52	0.66
1200	0.69	0.48	1530	0.50	0.58
1400	0.60	0.42	2040	0.30	0.39
1600	0.53	0.37			
1800	0.47	0.33			
2000	0.43	0.30			

the two values is excellent considering the differences in the methods employed. Our values are in the midrange of those reported by Tyrrell[19] of 1×10^{-3} to 6×10^{-3} min^{-1}.

Computer-generated response curves

The primary difficulty in using the mathematical model of the calorimetric response to electrical heating is that four time constants are required and only τ_m and τ_t can be measured experimentally. Values of τ_b and τ_w must be calculated as described earlier. Experimental and calculated values of τ_m are given in Table 2. This error probably results from the assumption that the Pai power series which is used for calculating velocity distribution in a pipe is valid for flow in a closed cylinder.

The theoretical output of the bridge circuit as a function of time is shown in Fig. 5 for an overall circuit gain of 100. The mathematical model does not give a completely satisfactory description of the transient regions of the main and anterior periods. The error is small, however, for the steady-state regions of both periods. For example, the experimental time constant is 6.3 sec when $\gamma_b = 4.92 \times 10^{-4}$°C sec^{-1}, $N_s = 430$ rpm, and $r_s = 1.63$ cm. The value predicted at 400 rpm is 6.6 sec. The predicted change in the circuit output, Δe_0, measured from start to the steady-

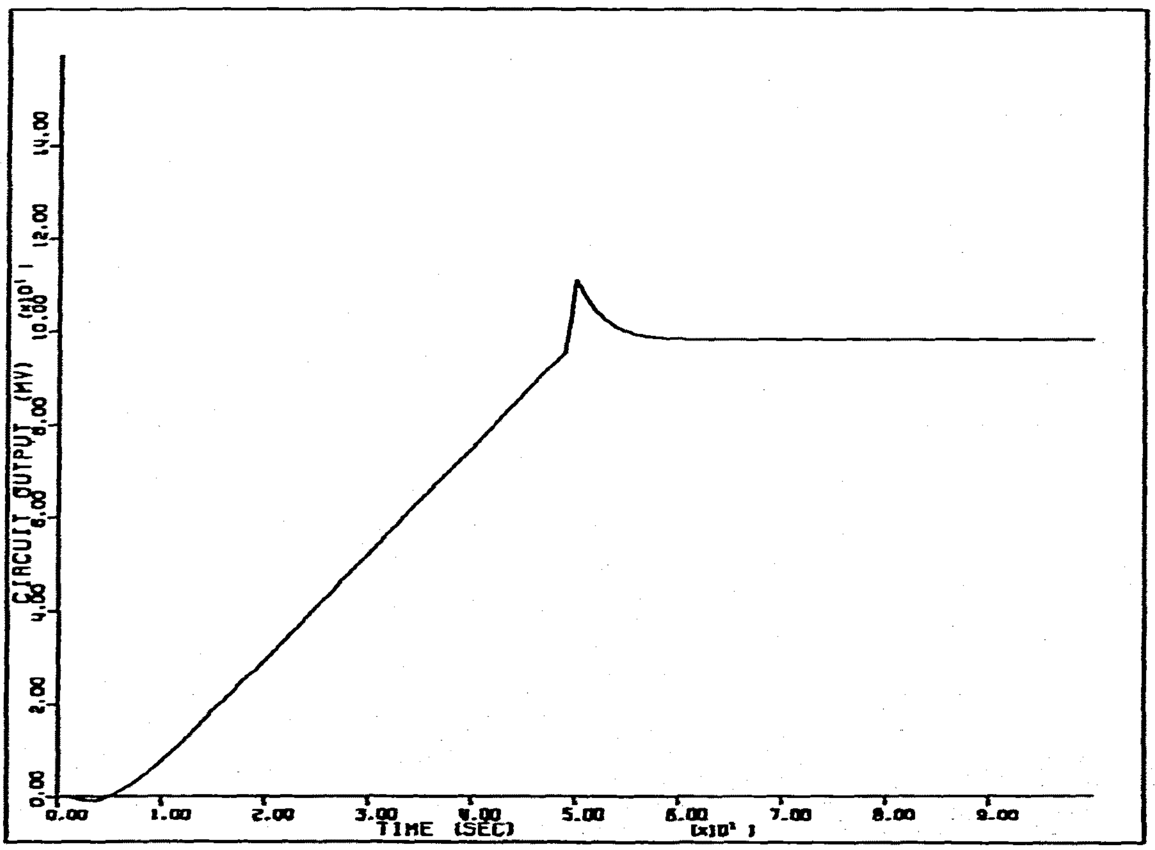

Fig. 5. Theoretical voltage output of the bridge circuit as a function of time. $N_s = 400$ rev min^{-1}.

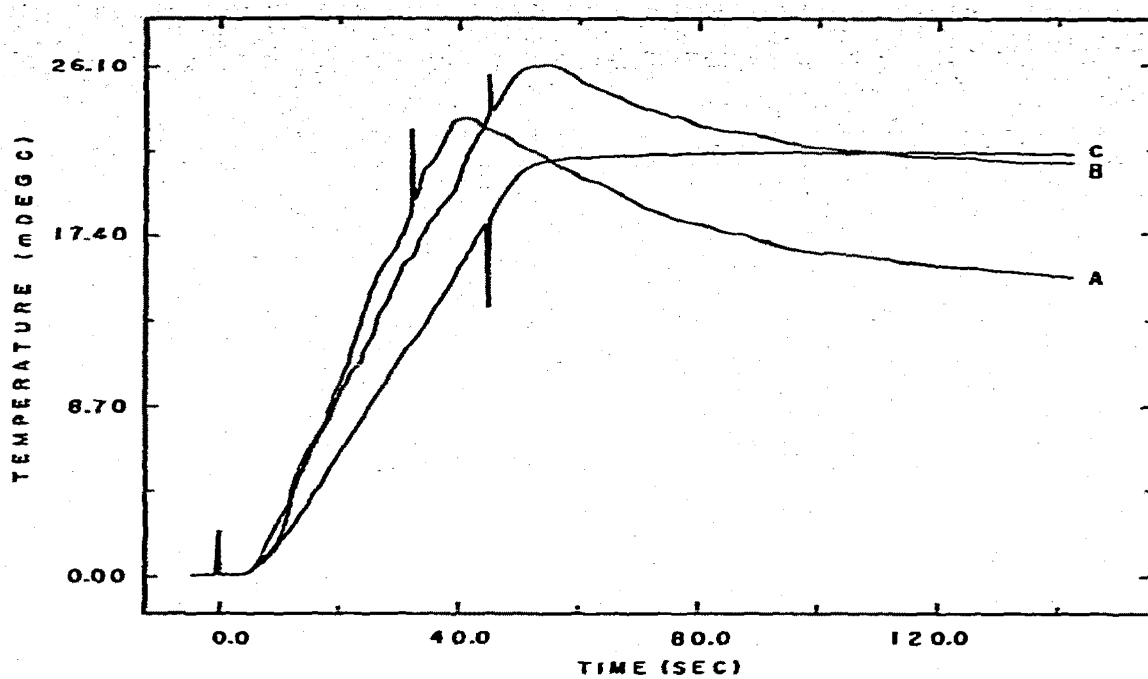

Fig. 6. Experimental heating curves of the reference cell as a function of r_s. N_s = 400 rev min^{-1}, e_+ = 1000.0 mV, e_- = 1000.2 mV, R_t = 1.056 mΩ and C_t = 0.047 μF; r_s: A = 0.64 cm, B = 1.27 cm, and C = 1.85 cm.

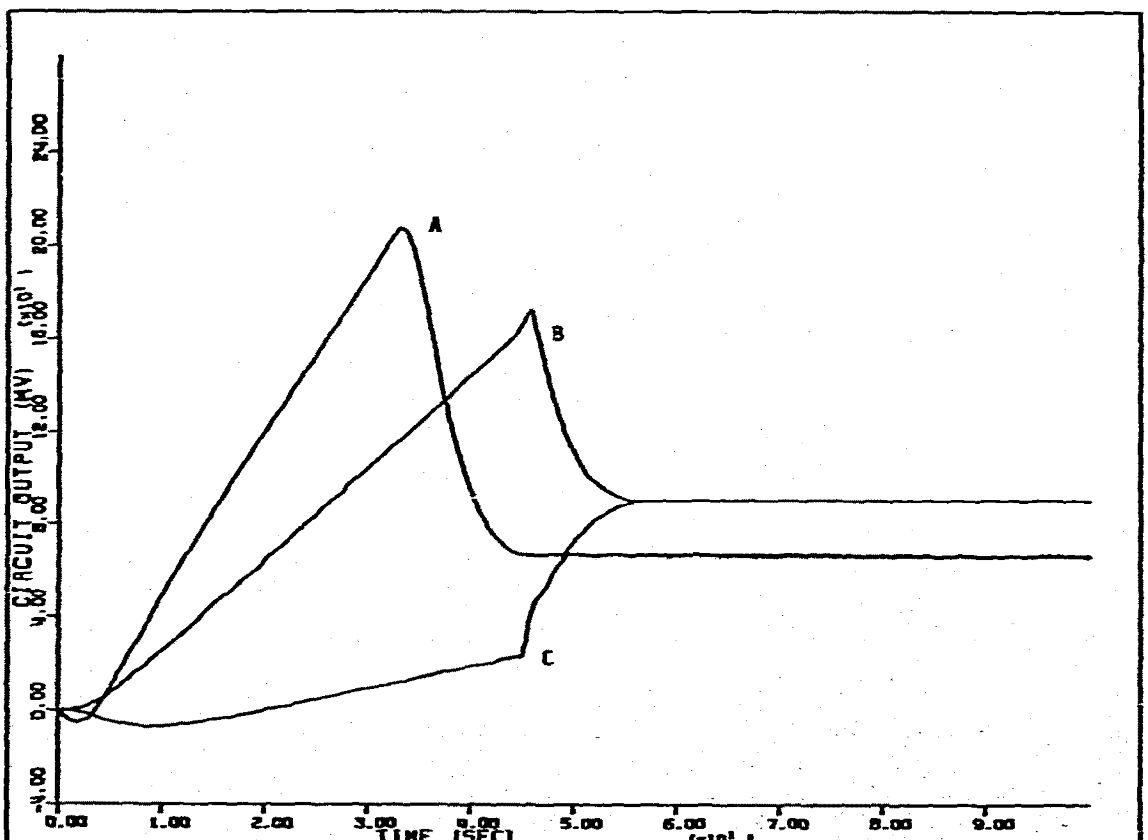

Fig. 7. Theoretical heating curves of the reference cell as a function of r_s. (Details as in Fig. 6.)

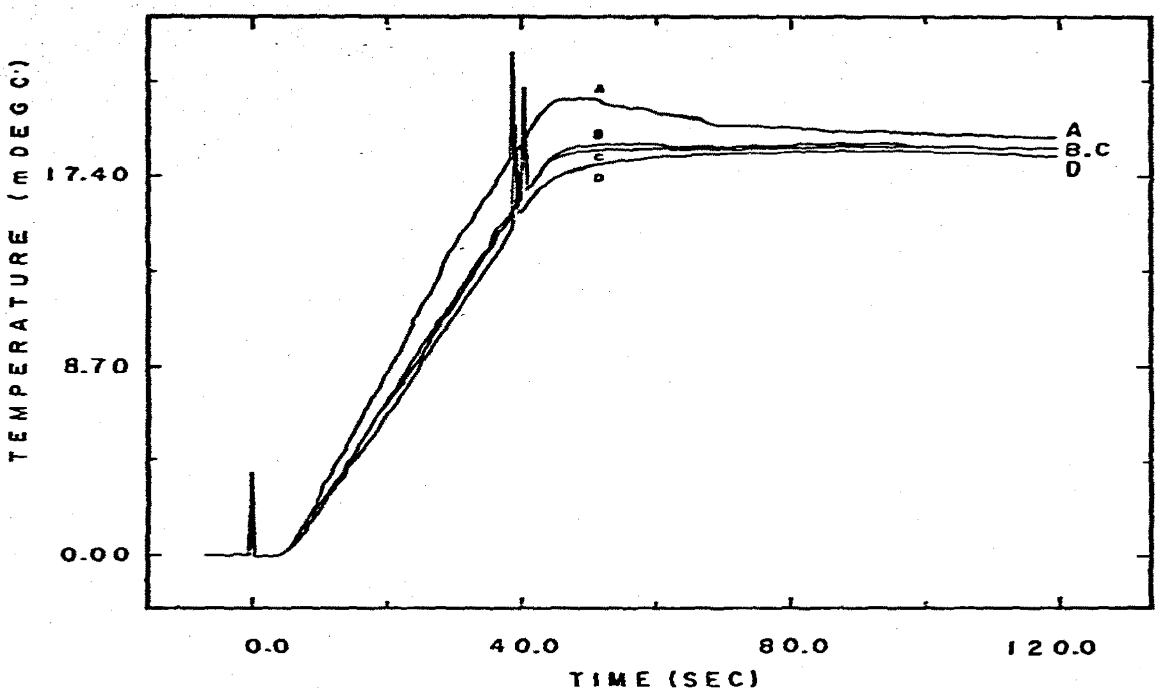

Fig. 8. Experimental heating curves of the reference cell as a function of N_s. r_s = 1.63 cm; e_+ = 1000.0 mV, e_- = 1000.2 mV, R_f = 1.056 M, and C_f = 0.047 μF; N_s: A = 400 rev min^{-1}, B = 800 rev min^{-1}, C = 1000 rev min^{-1} and D = 1980 rev min^{-1}.

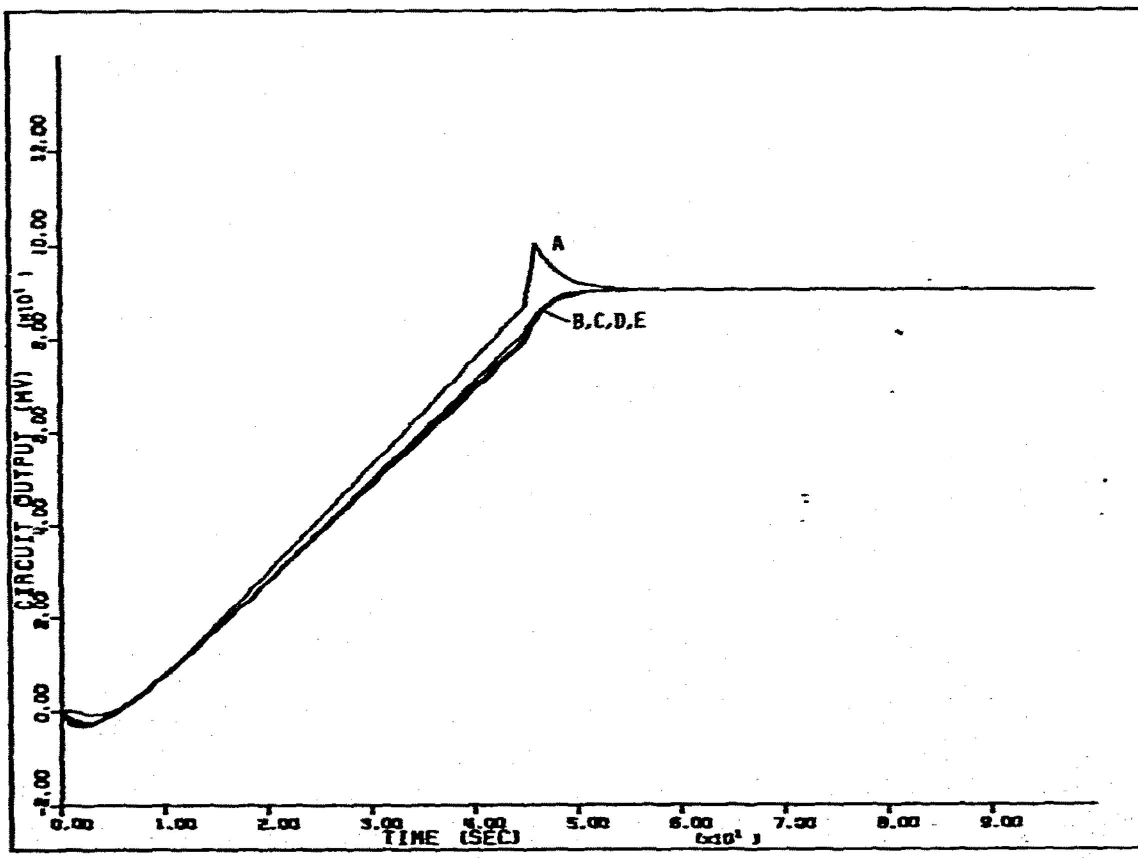

Fig. 9. Theoretical heating curves of the reference cell as a function of N_s. r_s = 1.63 cm; N_s: A = 400 rev min^{-1}, B = 800 rev min^{-1}, C = 1200 rev min^{-1}, D = 1600 rev min^{-1}, E = 2000 rev min^{-1}.

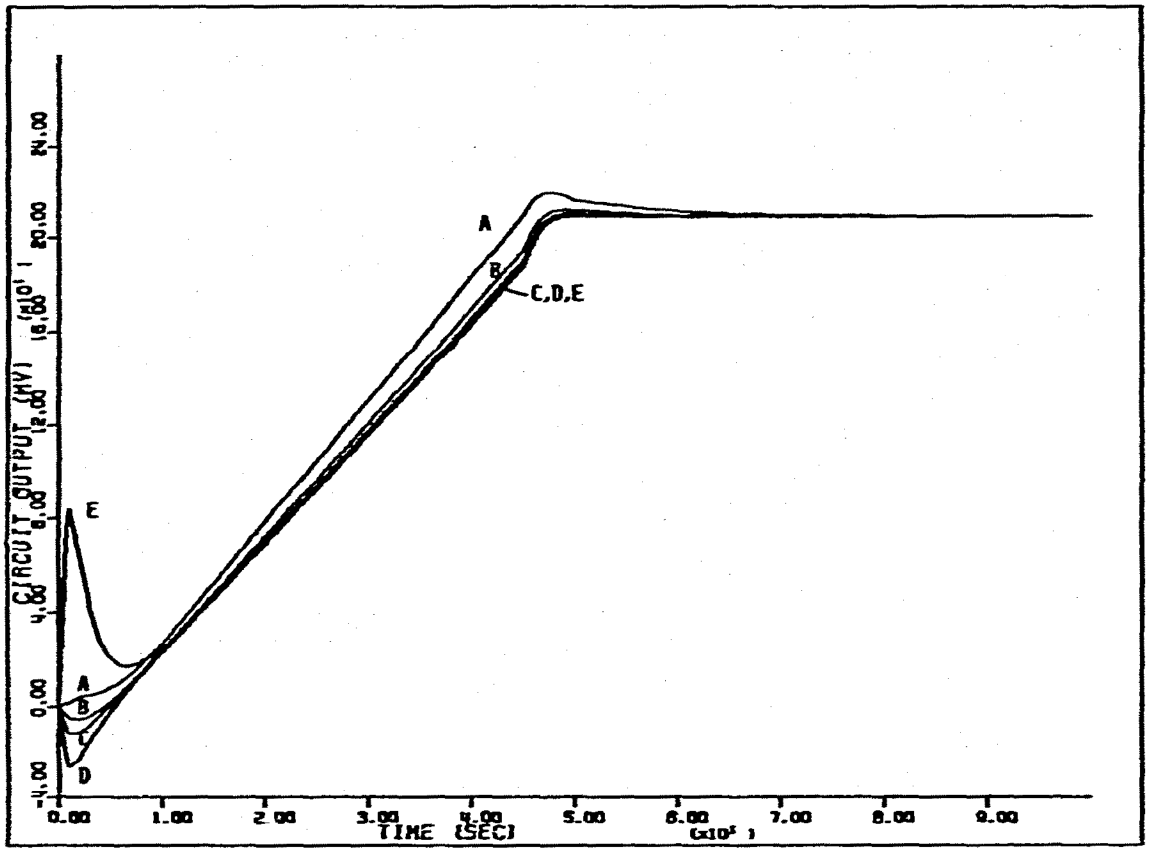

Fig. 10. Theoretical heating curves of the reference cell with toluene as the bulk solvent as a function of N_s. $r_s = 1.63$ cm; N_s: A = 400 rev min^{-1}, B = 800 rev min^{-1}, C = 1200 rev min^{-1}, D = 1600 rev min^{-1}, and E = 2000 rev min^{-1}.

state region of the anterior period is 98.44 mV. A value of 98.74 mV was observed experimentally for a heating time of 49 sec.

$T_h > T_b$ during electrical heating and the early portion of the anterior period before a steady-state temperature is reached. The location of the thermistor relative to the heater determines whether the thermistor is in a region of excess temperature ($T_{b,t} > T_{b,ave}$) or a region of deficient temperature ($T_{b,t} < T_{b,ave}$). When the thermistor is in a region of excess temperature, overshoot is observed at the point of heater cut-off, t_{co}. The temperature excess ($T_{b,t} - T_{b,ave}$) is in the order of 7 m°C for $\gamma_b = 4.92 \times 10^{-4}$°C sec^{-1}, $N_s = 200$ rpm, and $r_s = 1.63$ cm.

Experimental and theoretical heating curves are given in Figs. 6–9 for r_s = 0.64–1.85 cm. The curves illustrate dramatically that critical damping of a calorimeter can be achieved by proper choice of r_s and N_s. The conclusion of some workers[4, 6] that k becomes constant after 3 to 30 sec, dependent only on calorimeter design, is not supported by our results. Certainly C_w influences the response but it does not have the overwhelming importance commonly thought.

The effect of changing solvent was investigated by substituting toluene for water. The heating curves are shown in Fig. 10. The thermal conductivity and heat capacity of toluene are considerably different than those of water causing the extensive overshoot observed in Fig. 10. The sudden downward plunge of e_o after the start of the heating probably results from discarding the T_{bl} term in the derivation. The error is on the order of 2 m°C. All results shown were corrected throughout this work for the offset error calculated at $t = 0$. The complexity of the calorimetric system precludes an exact derivation including the R_{bl} term.

LIST OF SYMBOLS

$a, b, L, K, r, Z, \alpha, \beta, \xi, \psi, \theta, \sigma, \chi, \varepsilon$ coefficients

A_h	surface area of electrical heater (cm^2)
A_{stem}	area of mounting tubes in contact with bulk solution (cm^2)
A_w	surface area of calorimeter wall in contact with bulk solution (cm^2)
c_b	volume heat capacity of bulk solution (cal cm^{-3} °C^{-1})
c_p	mass heat capacity of bulk solution (cal g^{-1} °C^{-1})
C_b	heat capacity of bulk solution (cal °C^{-1})
c_{Cu}	mass heat capacity of copper metal (cal g^{-1} °C^{-1})
C_h	heat capacity of electrical heater (cal °C^{-1})
c_r	mass heat capacity of resistive element (cal g^{-1} °C^{-1})
C_w	heat capacity of calorimeter wall (cal °C^{-1})
γ_b	bulk solution heating rate (°C sec^{-1})
γ_{bkg}	heating rate of bulk solution by heat transferred through calorimeter wall from environment (°C sec^{-1})
γ_{str}	heating rate of bulk solution by stirring (°C sec^{-1})
γ_{th}	heating rate of bulk solution by thermistor (°C sec^{-1})
h_h	heat transfer coefficient of cylindrically shaped electrical heater (cal cm^{-2} sec^{-1} °C^{-1})
h_{hs}	heat transfer coefficient of heater stem (cal cm^{-2} sec^{-1} °C^{-1})
h_{stem}	heat transfer coefficient of heater, thermistor, mounting tubes, etc. (cal cm^{-2} sec^{-1} °C^{-1})
h_w	heat transfer coefficient of calorimeter (cal cm^{-2} sec^{-1} °C^{-1})
k	heat loss modulus
l_1	height of stirrer disc above the bottom of the calorimeter (cm)
l_2	depth of immersion of stirrer disc in bulk solution (cm)
l_b	depth of bulk solution (cm)
λ_b	thermal conductivity of bulk solution (cal cm^{-1} sec^{-1} °C^{-1})
λ_{Cu}	thermal conductivity of copper metal (cal cm^{-1} sec^{-1} °C^{-1})
λ_e	thermal conductivity of epoxy (cal cm^{-1} sec^{-1} °C^{-1})
λ_h	thermal conductivity of electrical heater (cal cm^{-1} sec^{-1} °C^{-1})
λ_r	thermal conductivity of metal film resistor (cal cm^{-1} sec^{-1} °C^{-1})
m_{Cu}	mass of copper sheath of electrical heater resistive element (g)
m_r	mass of electrical heater resistive element (g)

v_b	kinematic viscosity of bulk solution ($cm^2\ sec^{-1}$)
N_s	stirrer rotational speed ($rev\ min^{-1}$)
ω_s	angular velocity of stirrer ($rad\ sec^{-1}$)
P_h	electrical energy supplied for heating per unit time ($cal\ sec^{-1}$)
Q_h	heat supplied electrically to the calorimeter (cal)
r_c	radius of calorimeter cell (cm)
r_h	radius of electrical heater (cm)
r_s	radius of stirring disc (cm)
r_{sh}	radius of stirrer shaft (cm)
r_{stem}	average radius of mounting tubes (cm)
s	Laplacian operator
σ_s	dimensionless shielding parameter
t	time (sec)
T_b	temperature of bulk solution (°C)
T_{bl}	temperature of bulk solution at the interface of the bulk solution and electrical heater boundary layer (°C)
T_h	temperature of electrical heater (°C)
T_w	temperature of calorimeter wall (°C)
τ_h	time constant of electrical heater (sec)
τ_m	time constant of mixing (sec)
$\tau_{m,disc}$	time constant of mixing for stirrer disc (sec)
$\tau_{m,shaft}$	time constant of mixing for stirrer shaft (sec)
τ_w	time constant of calorimeter wall (sec)
$U_s(r)$	radial velocity of bulk fluid at distance r due only to stirrer disc ($cm\ sec^{-1}$)
$U_{sh}(r)$	radial velocity of bulk fluid at distance r due only to stirrer shaft ($cm\ sec^{-1}$)
$x_{e,h}$	thickness of epoxy coating an electrical heater (cm)
x_s	thickness of stirrer disc (cm)
x_{Cu}	thickness of copper tubing surrounding metal film resistor (cm)

REFERENCES

1 W. P. White, *The Modern Calorimeter*, Chemical Catalog Co., New York, 1928.
2 K. L. Churney, G. T. Armstrong and E. D. West, *Nat. Bur. Stand., Special Publication*, 338 (1970) 23.
3 H. A. Skinner, J. M. Sturtevant and S. Sunner, in H. A. Skinner (Ed.), *Experimental Thermochemistry*, Interscience, New York, 1962, p. 157.
4 S. Sunner and I. Wadsö, *Acta Chem. Scand.*, 13 (1959) 97.
5 J. J. Christensen, R. M. Izatt and L. D. Hansen, *Rev. Sci. Instrum.*, 36 (1965) 779.
6 *Tronac Thermometric Titration Calorimeter*, Tronac, Box 37, Orem, Utah 84057.
7 J. J. Christensen, H. D. Johnston and R. M. Izatt, *Rev. Sci. Instrum.*, 39 (1968) 1356.
8 C. E. Johansson, *Talanta*, 17 (1970) 739.
9 J. Polaczek and Z. Lisicki, *J. Therm. Anal.*, 3 (1971) 3.
10 R. S. Brodkey, *The Phenomena of Fluid Motions*, Addison-Wesley, London, 1967, p. 327.
11 A. E. Van Til, *Ph. D. Dissertation*, Iowa State University, Ames, Iowa 1976.
12 M. D. Scadron and I. Warshawsky, *Experimental Determination of Time Constants and Nusselt Numbers for Bare-Wire Thermocouples in High Velocity Air Streams and Analytic Approximation of Conduction and Radiation Errors*, NACA, TN 2599, Jan., 1952.

13 W. R. Bratschun, A. J. Mountvala and A. G. Pincus, *Uses of Ceramics in Microelectronics, A Survey*, NASA SP-5097, 1971, pp. 16–19.
14 A. Žukauskas, *Advances in Heat Transfer*, Academic Press, New York, 1972, p. 144.
15 S. Nagata, M. Nishikawa and T. Takimoto, *Heat-Japanese Res.*, 1 (1972) 49.
16 L. F. Ebell, *Anal. Chem.*, 37 (1965) 446.
17 S. Gunn, *J. Chem. Thermodyn.*, 3 (1971) 19.
18 W. Swietoslawski, *Microcalorimetry*, Reinhold, New York, 1946, p. 147.
19 H. J. V. Tyrrell and A. E. Beezes, *Thermometric Titrimetry*, Chapman and Hall, London, 1968, p. 25.
20 R. P. Tye (Ed.), *Thermal Conductivity*, Academic Press, London, 1969, p. 146.
21 R. C. Weast, Ed., *Handbook of Chemistry and Physics*, Chemical Rubber Publishing Co., Cleveland, Ohio, 47th ed., 1966–1967.
22 R. E. Treybal, *Mass-Transfer Operations*, McGraw-Hill, New York, 2nd Ed., 1968, p. 33.
23 R. C. Reid and T. K. Sherwood, *The Properties of Gases and Liquids*, McGraw-Hill, New York, 2nd Ed., 1966, p. 548.
24 Y. S. Touloukian and T. Makita, *Thermophysical Properties of Matter, Specific Heat. Nonmetallic Liquids and Gases*, Vol. 6, Plenum, New York, 1970, p. 285.